

# Dynamic and Steady State Modelling of the Brushless Doubly Fed Twin Stator Induction Generator with Core Loss

G. Boardman, J.G. Zhu, Q. P. Ha

Faculty of Engineering,  
University of Technology, Sydney  
PO. Box 123, Broadway 2007, Australia  
phone: ++612 9514 2338, fax: ++612 9514 2435, e-mail: gerard@eng.uts.edu.au

**Abstract.** This paper presents dynamic and steady state models of the brushless doubly fed twin stator induction machine (BDFTSIM) with emphasis on its use as a generator. The dynamic models are presented in the general reference frame. The models include the effects of core loss on both the stator and the rotor. The frequency on the rotor of the BDFTSIM is much higher than in a standard induction machine so that core losses can not be neglected. The performance analysis indicates the feasibility of the BDFTSIM as a variable speed wind generator

## Key words

Wind power generation, variable speed, modelling.

## 1. Introduction

Wind power is one of the renewable energy resources that have attracted most attention for a long time. For small power generation isolated from the grid, such as remote area power supplies, systems consisting of a single small power wind generator and a relatively simple and low cost power electronic controller are commonly used. For large scale grid connected power generation, however, wind farms consisting of a great number of large power wind, either synchronous or asynchronous, generators with much more sophisticated and expensive controllers are required.

When synchronous generators are used the converter has to be rated for the full capacity of the generator. The capacity of the converter can be reduced by using a doubly fed induction generator. In this case the converter has to process only a fraction of the VA of the machine. One disadvantage with classical wound rotor doubly fed induction machines is the need for maintenance of the slip ring brushgear.

Doubly fed induction machines have a great advantage in high power, variable speed generator applications because independent control of active and reactive power can be achieved by using a power electronic converter

connected to the rotor circuit so that it handles only a fraction of the total power [1],[2].

To combine this great advantage of doubly fed induction generators with high reliability and low maintenance requirements the BDFTSIM is being investigated. The major area for the application of the BDFTSIM is considered to be high power wind generators where variable speed operation, high reliability and low maintenance of the generators, which are placed on high towers, are important.

One of the benefits of the DFTSIM is it exhibits synchronous behaviour at a pre determined, user settable, variable speed using a variable frequency converter of fractional rating. The DFTSIM being studied consists of two wound rotor induction machines, shown schematically in Fig.1. The rotors of the machines are mechanically coupled and the rotor windings are connected so as to produce contra rotating magnetic fields in the separate machine sections. The fractionally rated converter is connected to the stator winding of the control machine.

Because the two rotors are physically coupled, as depicted in Fig. 1, permanent connections may be made, rendering the brushes redundant except for providing a convenient means of measuring the rotor quantities. Under these conditions the DFTSIM is brushless.

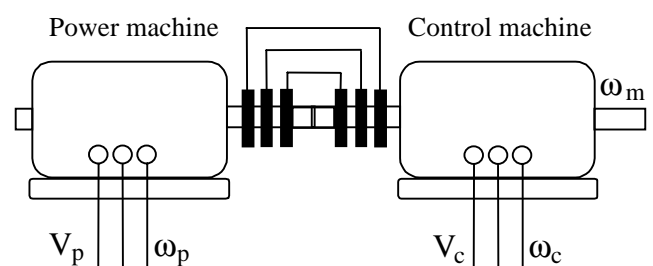


Fig.1 Arrangement of the BDFTSIM

A number of studies have been conducted on the performance modelling of the brushless doubly fed machine (BDFM) [3]-[5], which is functionally equivalent to the DFTSIM.

When the DFTSIM operates in the synchronous mode, there is a single frequency of current in the rotor, and the rotor speed is a simple function of the stator supply frequencies and numbers of pole pairs, as follows:

$$N_m = 60 (f_p + f_c) / (P_p + P_c) \quad (1)$$

The natural speed,  $N_n$ , occurs when dc is applied to the control winding.

The control machine is used to regulate both the active and reactive power being output by the power machine in generating mode. The nomenclature used in the paper is given in the Appendix.

## 2. Dynamic Modelling

The BDFTSIM comprises two induction machines with their rotors inter connected electrically and coupled mechanically. The power and control windings are respectively the power machine and control machine stator windings.

### A. General Assumptions

The following assumptions are made:

- 1) Balanced three phase windings are distributed to produce sinusoidal flux density;
- 2) Only the fundamental components of voltage and current are considered;
- 3) Zero sequence quantities are not present.

### B. Dynamic Voltage Equations of Induction Machine

There are many possible methods for calculating the transient performance of electrical machines, including matrix calculation. The space vector method is a simple but mathematically precise method that allows the physical phenomena of the machine to be seen. The space vector concept is a mathematical abstraction that is useful in the study of electrical machines. The voltage and flux linkage space vectors are related to the flux density,  $\mathbf{B}$ , which is a vector quantity. The current space vector is related to the m.m.f. which in turn is related to another vector quantity, the magnetic field intensity,  $\mathbf{H}$ .

The two-axis theory of the three phase induction motor is well developed and is used as the starting point for the development of the dynamic equations of the BDFTSIM. The dynamic voltage equation of the power machine, in the general reference frame, is written as:

$$\begin{bmatrix} \mathbf{v}_s^g \\ \mathbf{v}_r^g \end{bmatrix} = \begin{bmatrix} R_s + (p + j\omega_g)L_s & (p + j\omega_g)L_m \\ (p + j(\omega_g - \omega_r))L_m & R_r + (p + j(\omega_g - \omega_r))L_r \end{bmatrix} \begin{bmatrix} \mathbf{i}_s^g \\ \mathbf{i}_r^g \end{bmatrix} \quad (2)$$

where

$$\begin{aligned} \mathbf{v}_s^g &= \mathbf{v}_s e^{-j\theta_g}, \quad \mathbf{v}_r^g = \mathbf{v}_r e^{-j(\theta_g - \theta_r)}, \\ \mathbf{i}_s^g &= \mathbf{i}_s e^{-j\theta_g}, \quad \mathbf{i}_r^g = \mathbf{i}_r e^{-j(\theta_g - \theta_r)}, \\ \mathbf{v}_s &= 2/3 (v_{sa}(t) + \mathbf{a}v_{sb}(t) + \mathbf{a}^2v_{sc}(t)), \\ \mathbf{v}_r &= 2/3 (v_{ra}(t) + \mathbf{a}v_{rb}(t) + \mathbf{a}^2v_{rc}(t)), \\ \mathbf{i}_s &= 2/3 (i_{sa}(t) + \mathbf{a}i_{sb}(t) + \mathbf{a}^2i_{sc}(t)), \\ \mathbf{i}_r &= 2/3 (i_{ra}(t) + \mathbf{a}i_{rb}(t) + \mathbf{a}^2i_{rc}(t)), \quad \theta_r = P_p \theta_m \end{aligned}$$

The instantaneous electromagnetic torque is

$$\tau_e = 3/2 P_p \Psi_s^g \times \mathbf{i}_s^g = 3/2 P_p L_m \mathbf{i}_r^g \times \mathbf{i}_s^g \quad (3)$$

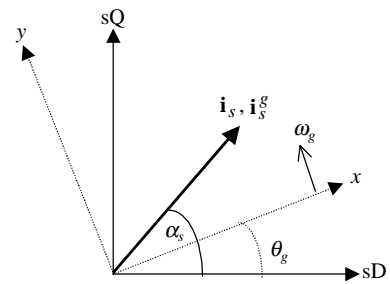
where

$$\Psi_s^g = L_s \mathbf{i}_s^g + L_m \mathbf{i}_r^g$$

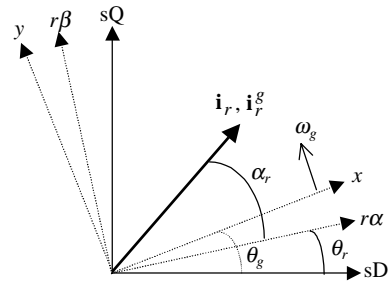
The space vectors  $\mathbf{v}_s$  and  $\mathbf{i}_s$  are respectively the stator voltage and stator current in the stator reference frame. The space vectors  $\mathbf{v}_r$  and  $\mathbf{i}_r$  are respectively the rotor voltage and current in the rotor reference frame. To analyse the machine it is necessary to have a common reference frame for the stator and rotor quantities. This is the only way to overcome the mathematical and physical difficulties of discussing their interactions and of finding simple solutions for the relevant differential equations. The transformation of the stator and rotor current space vectors from their natural reference frames to the general reference frame is depicted in Fig. 2.

### C. Formation of BDFTSIM

The BDFTSIM is formed by mechanically coupling two induction machines and interconnecting their rotor windings. The interconnections require that the magnetic fields on the two rotor sections rotate in opposite directions. Two interconnections that produce contra rotating fields on the rotor are shown in Fig. 3; one with the machines coupled facing the same direction, the other with the machines facing each other, as depicted in Fig. 1.

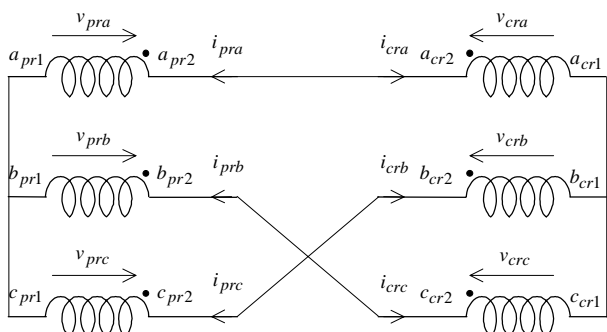


(a) Transformation of the stator current

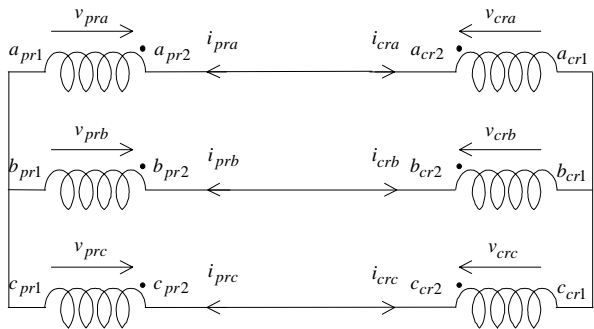


(b) Transformation of the rotor current

Fig.2 Application of the general reference frame



(a) Machines coupled facing the same direction



(b) Machines coupled facing back-to-back

Fig. 3 Interconnection of rotor windings to produce contra rotating fields on rotor windings

With the machines coupled and interconnected in Fig. 3(a) the rotor current and voltage space vectors are related as

$$\mathbf{i}_{cr} = -\mathbf{i}_{pr}^*, \quad \mathbf{v}_{cr} = -\mathbf{v}_{pr}^* \quad (4)$$

With the machines coupled and interconnected in Fig. 3(b) the rotor current and voltage space vectors are related as

$$\mathbf{i}_{cr} = \mathbf{i}_{pr}^*, \quad \mathbf{v}_{cr} = \mathbf{v}_{pr}^* \quad (5)$$

There are many ways in which the two rotor windings may be connected to form the BDFTSIM [6]. The general form of the relationship between the rotor current and voltage space vectors is

$$\mathbf{i}_{cr} = (\mathbf{i}_{pr} e^{j\varphi})^* \quad \text{and} \quad \mathbf{v}_{cr} = -(\mathbf{v}_{pr} e^{j\varphi})^* \quad (6)$$

where  $\varphi$  is related to the method of interconnection and any angular misalignment of the two rotors [6].

The conjugation in (4), (5) and (6) is a consequence of the requirement that there be contra rotating fields on the two rotor sections.

$$\begin{bmatrix} \mathbf{v}_p^g \\ (\mathbf{v}_c^g e^{j\theta_h})^* \\ 0 \end{bmatrix} = \begin{bmatrix} R_{ps} + (p + j\omega_g)L_{ps} & 0 & (p + j\omega_g)L_{pm} \\ 0 & R_{cs} + (p + j(\omega_g - P_p\omega_m - P_c\omega_m))L_{cs} & (p + j(\omega_g - P_p\omega_m - P_c\omega_m))L_{cm} \\ (p + j(\omega_g - P_p\omega_m))L_{pm} & (p + j(\omega_g - P_p\omega_m))L_{cm} & R_r + (p + j(\omega_g - P_p\omega_m))L_r \end{bmatrix} \begin{bmatrix} \mathbf{i}_p^g \\ (\mathbf{i}_c^g e^{j\theta_h})^* \\ \mathbf{i}_{pr}^g \end{bmatrix} \quad (7)$$

Without loss of generality the coupling and interconnection shown in Fig. 3(b) will be assumed. Under these conditions the dynamic voltage equations for the BDFTSIM, in the general reference frame, are shown in (7) [6]. In (7)  $R_r = R_{pr} + R_{cr}$  and  $L_r = L_{pr} + L_{cr}$  and

$$\theta_h = 2\theta_g - P_p\theta_m - P_c\theta_m \quad (8)$$

is the angle that maps the control machine quantities on to the same reference frame as the power machine quantities.

The electromagnetic torque is the sum of the contributions from the power and control machine sections and is

$$\tau_e = 3/2 P_p L_{pm} \Im(\mathbf{i}_{ps}^g \mathbf{i}_{pr}^{g*}) + 3/2 P_c L_{cm} \Im(\mathbf{i}_{cs}^g \mathbf{i}_{pr}^g) \quad (9)$$

The first term of (9) represents the torque contributed by the power machine and the second the torque contributed by the control machine.

#### D. Core loss modelling

In an induction machine under normal running conditions the slip is low and the core loss may be neglected. In the BDFTSIM this is not the case, for the BDFTSIM under consideration the rotor electrical frequency may be greater than 30 Hz and thus core loss cannot be neglected without loss of accuracy.

The accurate calculation of core loss is complicated and only a simple treatment is included in this paper [8]. The three elements of core loss are hysteresis, eddy current and anomalous losses. The total loss may be expressed in the following form

$$\wp^{fe} = k_h \omega \Psi_m^n + k_e \omega^2 \Psi_m^2 + k_a \omega^{1.5} \Psi_m^{1.5} \quad (10)$$

where  $k_h$ ,  $k_e$  and  $k_a$  are hysteresis, eddy current and anomalous loss constants respectively that vary according to the type and grade of lamination and  $n$  is the Steinmetz constant ( $\approx 1.5 < n < 2.5$ ).

The hysteresis loss is proportional to the electrical frequency and the eddy current loss is proportional to the square of the electrical frequency. The BDFTSIM has two stator windings that carry, in general, different frequencies of current. The rotor winding has a single frequency of current that is different from that of the two stator windings

It is clear, from (10) that the eddy current loss will dominate at high frequencies. If, in the first instance, the hysteresis loss and anomalous losses are neglected the iron loss on the power winding stator is

$$\varphi_{ps}^{fe} \approx k_{es} \omega_p^2 \Psi_{pm}^2 \quad (11)$$

The power machine stator winding frequency,  $\omega_p$ , is fixed at the frequency of the utility. The quantity  $1/k_e$  has the dimension of resistance. In this form, (11) may be modelled in the classical form as a resistance in parallel with the magnetizing inductance and the value of the resistance is

$$R_{ps}^{fe} = 1/k_{es} \quad (12)$$

The electrical frequency on the rotor is at slip frequency,  $s_r$ , and so the iron loss on the power machine rotor is

$$\varphi_{pr}^{fe} \approx k_{er} s_r^2 \omega_p^2 \Psi_{pm}^2 \quad (13)$$

The equivalent core loss resistance modelled on (13) is a function of the machine slip and the power loss may be written as

$$\varphi_{pr}^{fe} \approx \left( \omega_p^2 \Psi_{pm}^2 \right) / \left( k_{er} / s_r^2 \right) \quad (14)$$

There are similar, frequency dependent, losses on the control machine rotor and stator.

The impedance matrix of (7) is of order 3x3. If the iron losses are incorporated into the model the impedance matrix increases to order 7x7. The impedance matrix may be reduced to 3x3 after considerable manipulation if the following substitutions are made to (7)

$$\begin{aligned} L_{ps} &\rightarrow L_{ps}^{fe}, & L_{pm} &\rightarrow L_{pm}^{fe}, & L_{cs} &\rightarrow L_{cs}^{fe}, \\ L_{cm} &\rightarrow L_{cm}^{fe}, & L_r &\rightarrow L_r^{fe} \end{aligned} \quad (15)$$

where

$$\begin{aligned} L_{ps}^{fe} &= L_{pls} + L_{pm}^{fe}, & L_{cs}^{fe} &= L_{cls} + L_{cm}^{fe}, \\ L_r^{fe} &= L_{pr}^{fe} + L_{cr}^{fe} = L_{plr} + L_{pm}^{fe} + L_{clr} + L_{cm}^{fe} \end{aligned}$$

The new inductance terms in (15) are

$$L_{pm}^{fe} = \frac{L_{pm} R_{ps}^{fe} R_{pr}^{fe} / s_r^2}{R_{ps}^{fe} \frac{R_{pr}^{fe}}{s_r^2} + (p + j\omega_g) L_{pm} \frac{R_{pr}^{fe}}{s_r^2} + (p + j\omega_g - j\omega_r) L_{pm} R_{ps}^{fe}} \quad (16)$$

and

$$L_{cm}^{fe} = \frac{L_{cm} \left( R_{cs}^{fe} / s^2 \right) \left( R_{cr}^{fe} / s_r^2 \right)}{\frac{R_{cs}^{fe}}{s^2} \frac{R_{cr}^{fe}}{s_r^2} + \frac{R_{cr}^{fe}}{s_r^2} (p + j(\omega_g - (p_p + p_c) \omega_m)) L_{cm} + \frac{R_{cs}^{fe}}{s^2} (p + j\omega_g - j\omega_r) L_{cm}} \quad (17)$$

In (16) and (17) the values of the core loss resistances, denoted by the superscript  $fe$ , are the equivalent resistance values calculated at 50 Hz.

By neglecting the hysteresis and anomalous losses in (10) the iron loss is proportional to the square of both the magnitude of the revolving field and its angular velocity and it may be modelled simply by an equivalent resistance the value of which is proportional to the square of the slip.

If the hysteresis and anomalous losses are included this simple resistance model is inadequate. To keep the model relatively simple but to incorporate the effects of hysteresis the iron loss is assumed to be

$$\varphi_{50}^{fe}(s) \approx s^{1.3} \varphi_{50}^{fe} \quad (18)$$

where  $\varphi_{50}^{fe}$  is the value of the iron loss when measured at the utility frequency and  $s$  is the relevant slip. The factor 1.3 is an empirical factor. Under these conditions the exponent of the slip related to the core loss resistance values in (16) and (17) is 1.3 and not 2.

When the effects of core loss are modelled the stator currents carry a component of current necessary to support the core loss and as a consequence, the electromagnetic torque of (9) needs to be modified. One of the advantages with the substitutions for the inductance made in (15) is that the electromagnetic torque may be written in terms of the stator currents, which can be measured directly, with the relevant inductance again replaced by its new value calculated in accordance with (16) or (17) as appropriate.

The electromagnetic torque with core loss is

$$\tau_e = 3/2 P_p L_{pm}^{fe} \Im \left( \mathbf{i}_{ps}^g \mathbf{i}_{pr}^{g*} \right) + 3/2 P_c L_{cm}^{fe} \Im \left( \mathbf{i}_{cs}^g \mathbf{i}_{pr}^g \right) \quad (19)$$

The equivalent circuit shown in Fig. 4 may represent the voltage equation in (7) with the modified inductance values and the equivalent circuits in Fig. 5 may represent the modified inductance values.

### 3. Steady State Modelling

The foregoing equations are valid for all input voltages including dc and all ac waveforms. With sinusoidal excitation on the power and control windings

$$\mathbf{v}_{ps}^g = \sqrt{2} V_{ps} e^{j(\theta_p - \theta_g)}, \quad \mathbf{v}_{cs}^{g*} = \sqrt{2} V_{cs} e^{-j(\theta_c - \theta_g)} \quad (20)$$

For the BDFTSIM to exhibit synchronous behaviour the frequency of the current induced in both the power machine rotor and the control machine rotor must be the same. Under these conditions

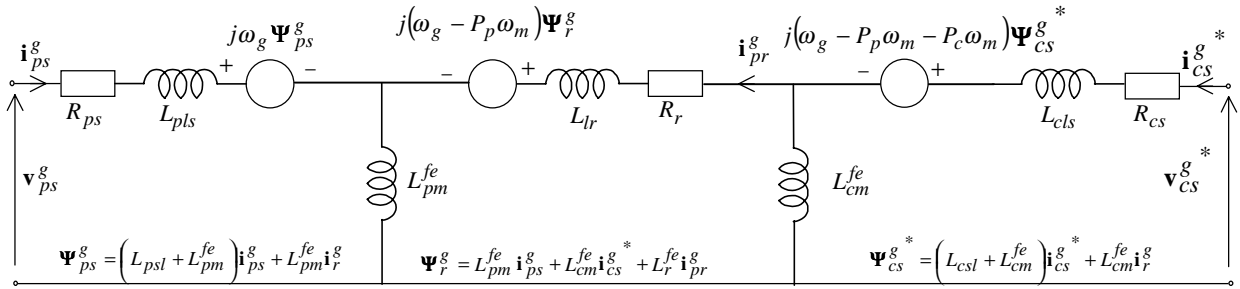


Fig. 4 Equivalent circuit of the BDFTSIM in the general reference frame

$$\theta_c = (P_p + P_c) \theta_m - \theta_p \quad (21)$$

When operating in synchronous mode the speed is

$$\omega_m = \frac{\omega_p + \omega_c}{P_p + P_c} \quad (22)$$

In the steady state the differential operator is

$$p = j(\omega_p - \omega_g) \quad (23)$$

Application of (22) to (7) and (9) gives the per phase steady state equations of the BDFTSIM as

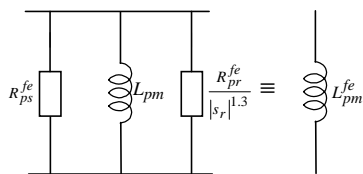
$$[\mathbf{V}] = [\mathbf{Z}][\mathbf{I}] \quad (24)$$

where

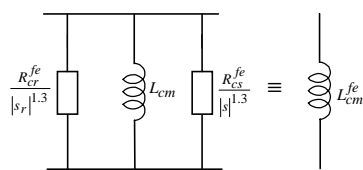
$$[\mathbf{V}] = \begin{bmatrix} \mathbf{V}_p & \mathbf{V}_c^* / s & 0 \end{bmatrix}^T, [\mathbf{I}] = \begin{bmatrix} \mathbf{I}_p & \mathbf{I}_c^* & \mathbf{I}_r \end{bmatrix}^T$$

$$[\mathbf{Z}] = \begin{bmatrix} (R_{ps} + jX_{ps}^{fe}) & 0 & jX_{pm}^{fe} \\ jX_{pm}^{fe} & (R_{cs}/s + jX_{cs}^{fe}) & jX_{cm}^{fe} \\ jX_{pm}^{fe} & jX_{cm}^{fe} & (R_r/s_r + jX_r^{fe}) \end{bmatrix}$$

$$X_{pm}^{fe} = \frac{\omega_p L_{pm} R_{ps}^{fe} s_r R_{pr}^{fe} / |s_r|^{1.3}}{R_{ps}^{fe} \frac{s_r R_{pr}^{fe}}{|s_r|^{1.3}} + j\omega_p L_{pm} \frac{s_r R_{pr}^{fe}}{|s_r|^{1.3}} + j\omega_p L_{pm} R_{ps}^{fe}}$$



(a) Power machine



(b) Control machine

Fig. 5 Modified inductance with core loss

$$X_{cm}^{fe} = \frac{\omega_p L_{cm} s \left( R_{cs}^{fe} / |s|^{1.3} \right) \left( s_r R_{cr}^{fe} / |s_r|^{1.3} \right)}{\frac{s R_{cs}^{fe}}{|s|^{1.3}} \frac{s_r R_{cr}^{fe}}{|s_r|^{1.3}} + j\omega_p L_{cm} \frac{s_r R_{cr}^{fe}}{|s_r|^{1.3}} + j\omega_p L_{cm} \frac{s R_{cs}^{fe}}{|s|^{1.3}}}$$

$$s_r = \frac{\omega_r}{\omega_p} \text{ and } s = -\frac{\omega_c}{\omega_p}$$

The equivalent circuit in Fig.5 may represent (24)

The magnitude of the steady state electromagnetic torque is

$$T_e = 3P_p L_{pm}^{fe} \Im(\mathbf{I}_p \mathbf{I}_r^*) + 3P_c L_{cm}^{fe} \Im(\mathbf{I}_c \mathbf{I}_r) \quad (25)$$

## 4. Performance Study

### A. Machine parameters

The machine parameters used in the simulations were those of a pair of laboratory machines with wound rotor,  $\Delta/Y$  connected, 4 pole, 22.5 kW, 240 Nm, 415 V 50 Hz, 40 A. The parameters of the machines, estimated off line, on a per phase basis are as follows:  $R_s=0.205 \Omega$ ,  $R_r=0.205 \Omega$ ,  $X_{ls}=0.67 \Omega$ ,  $X_{lr}=0.67 \Omega$ . The core loss resistances, calculated at 50 Hz are 308  $\Omega$  and 890  $\Omega$  for the stator and rotor respectively. The control machine is used to regulate both the active and reactive power flow it does not work in the constant flux mode. An allowance was made for saturation in the magnetizing inductance [8]

### B. Steady State Generating Performance

A number of papers have been published recently detailing the control and dynamic aspects of the BDFTSIM [3]-[5]. This performance study is restricted to a comparison of the steady state generating performance in two speed ranges; 400-1100 rpm, sub synchronous, and 1700-2225 rpm, super synchronous. All energy transfer in the BDFTSIM is by induction action even though the machine exhibits synchronous behaviour in that it can supply varying loads at fixed speed. As a consequence, no power can be generated at the synchronous speed of the power machine, 1500 rpm, and very little can be generated close to this speed.

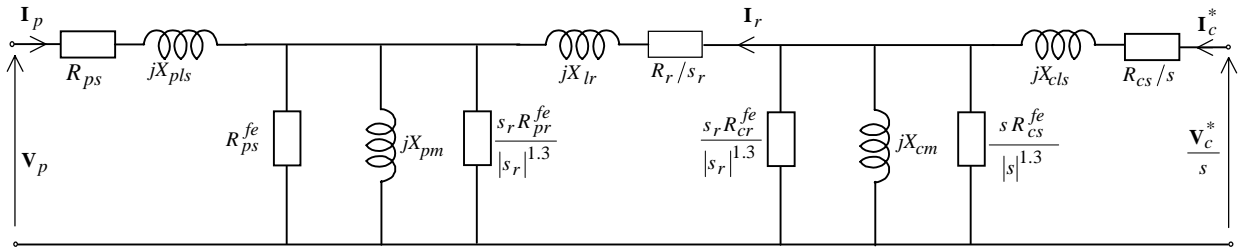


Fig. 5 Per phase steady state equivalent circuit of the BDFTSIM with core loss

### C. Sub Synchronous Operation

Some aspects of the performance of the BDFTSIM when the power machine is generating 20 kW in the speed range 400-1100 rpm are shown in Fig. 6. The power winding voltage is fixed at 240 V and the control winding voltage varies almost linearly with a minimum close to 750 rpm, the speed at which the control winding frequency is zero.

The magnitudes of the power and control winding currents are shown in Fig. 6(b). When the power machine generates at 0.8 pf lagging the currents are all within the 40 A rating. If the power factor of the power machine is increased to unity the control machine current is excessive, it is 46 A at 400 rpm and rises to over 50A at 1100 rpm. The situation becomes even worse if the power machine is operated at leading power factor, the control winding current is in excess of 60 A for 0.9 pf leading.

The magnitudes of the magnetizing flux shown in Fig. 6(c), which take into account saturation effects, indicate that the control machine is heavily saturated when the power winding operates at unity power factor. Even when operating at 0.8 pf lagging the control winding is saturated for speeds in excess of 750 rpm. The higher the speed the greater is the degree of saturation. It is noted that this tendency for the control winding to saturate is more pronounced at sub synchronous speeds in generating mode. When the BDFTSIM is operated as a motor the saturation effect is much lower in the sub synchronous speed range.

The output powers shown in Fig. 6(d) show that at both power factors the control machine acts as a motor at speeds below 750 rpm. The power being generated by the power machine is being circulated back to the control machine. At 400 rpm the control machine consumes around 12 kW of the 20 kW generated by the power machine. As a consequence the efficiency at low speeds is very low under these operating conditions. The efficiency improves the greater the speed, reaching over 85% for speeds in excess of 1000rpm. At this speed the power and VA is about the same as that at 500 rpm but this time the powers are aiding and the total output of the machine is around 30 kW, which is still below the combined power rating of the two component machines.

### D. Super Synchronous Operation

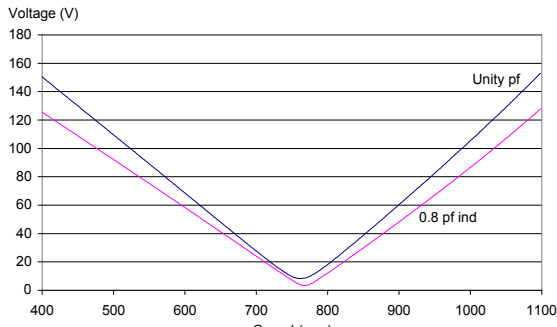
Operating the BDFTSIM at close to the natural speed, 750 rpm for this machine set, gives the minimum VA rating of the control winding converter. The reason for this is that the control winding voltage is relatively low. Except at speeds close to synchronous speed, where operation is impractical, the magnitude of the control winding current exceeds that of the power winding. This means that the converter devices must have a full current rating.

Operation at super synchronous speed means the control winding voltage is higher but there are several advantages to operation at super synchronous speed. To compare operation at sub and super synchronous speeds Fig. 7 shows the equivalent data to that shown in Fig. 6 for operation at sub synchronous speeds. The differences are that now the power machine output has been reduced to -18 kW and the speed range has been reduced. The differences are remarkable. The magnitude of the control winding voltage rises from around 200 V at 1700 rpm to over 400 V at 2250 rpm when the power machine is operating at 0.8 pf lagging. Operation at unity power factor causes the voltages to increase significantly. Apart from the magnitude of the control winding voltage, which is undesirably high, all the other indices are better at super synchronous speed.

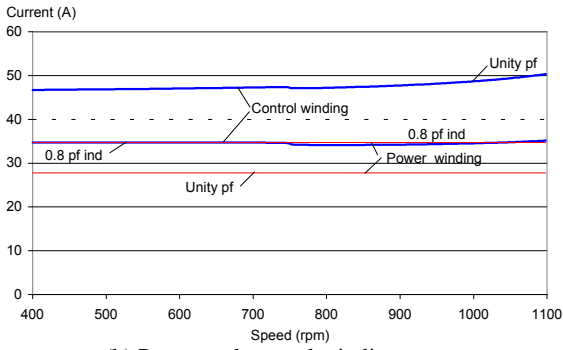
The power and control winding currents, shown in Fig. 7(b), indicate that, even at unity power factor, the currents are always below the 40 A rating. In terms of current rating it is possible to operate at leading power factor.

The magnitudes of the magnetizing fluxes, shown in Fig. 7(c) are greatly different from those at sub synchronous speed. In this case the control machine is not saturated, even when operating at unity power factor. This is a feature of the BDFTSIM. The corollary of this is that when operated as a motor at super synchronous speeds the BDFTSIM saturates even at modest loads. This is not a problem because it is impractical to operate the BDFTSIM under these motoring conditions because of the torque null at synchronous speed.

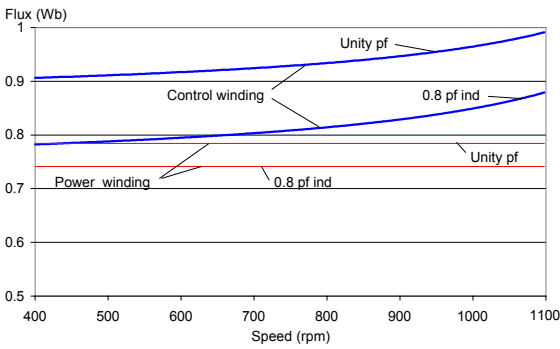
The output powers, shown in Fig. 7(d), indicate that just below 2000 rpm the full power capacity of the BDFTSIM can be realized. At all super synchronous speeds the control machine output aids the power machine output. The output from the power machine exceeds that of the power machine for speeds in excess of about 1800 rpm.



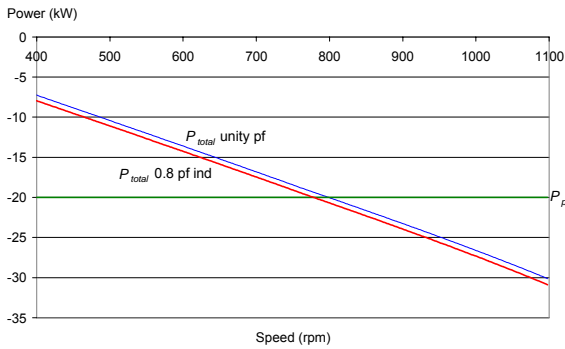
(a) Control winding voltage



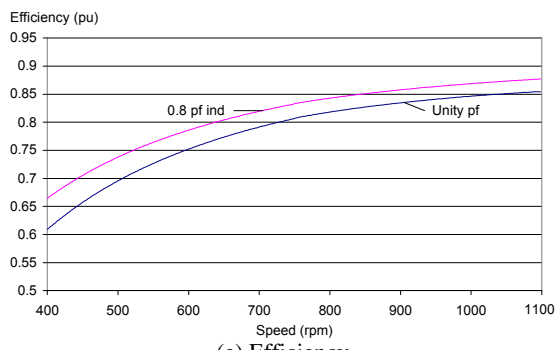
(b) Power and control winding currents



(c) Power and control magnetizing flux

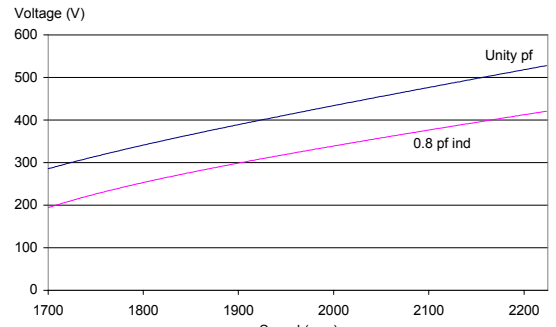


(d) Output power

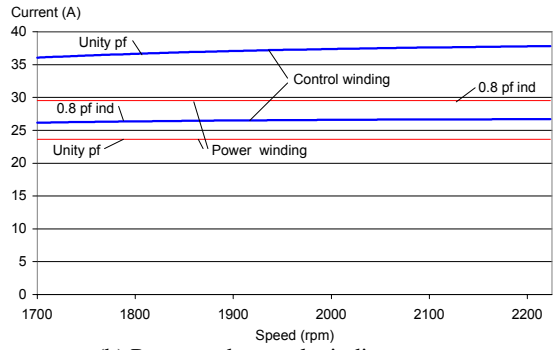


(e) Efficiency

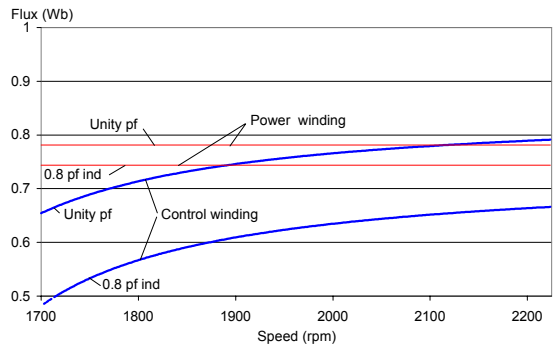
Fig. 6 Sub synchronous operation,  $P_p = -20$  kW



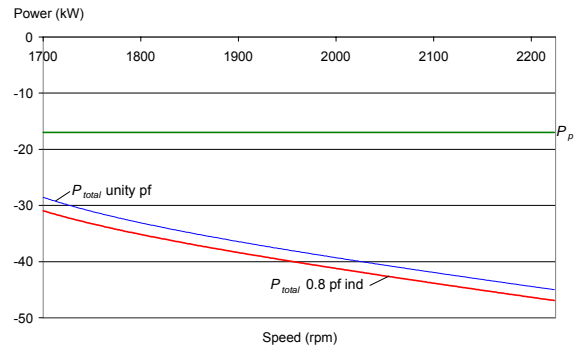
(a) Control winding voltage



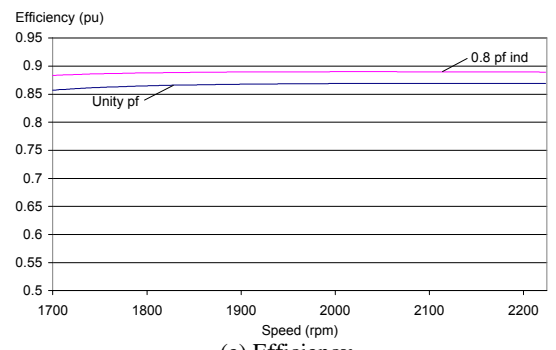
(b) Power and control winding currents



(c) Power and control magnetizing flux



(d) Output power



(e) Efficiency

Fig. 7 Super synchronous operation,  $P_p = -17$  kW

Because the two output power components aid and the currents are not excessive the efficiency in super synchronous mode is relatively high, as shown in Fig. 7(e). Even allowing for core loss and saturation the efficiency is always above 85%. The magnitudes of the currents are more balanced at 0.8 pf and so the efficiency is consistently higher than at unity power factor operation.

#### 4. Conclusion

A model of the BDFTSIM has been presented that includes the effects of core loss. The model covers both dynamic and steady state operation. Based on the model a study has been carried out on the steady state performance of the BDFTSIM as a generator in both sub and super synchronous speed ranges.

The BDFTSIM is a viable alternative to both doubly fed induction generators and variable speed synchronous generators, particularly in wind powered applications. The BDFTSIM requires a converter of fractional rating, unlike a variable speed synchronous generator which requires a fully rated converter. The rating of the BDFTSIM converter is dependent on the speed of operation. The BDFTSIM is brushless, unlike a doubly fed induction machine, and hence the maintenance requirement is much lower. The control machine acts as both to control the output of the power machine and to provide a significant proportion of the total power output.

At sub synchronous speed the rating of the converter is low, especially around the natural speed, primarily because of the low control winding voltage. The efficiency improves with increasing speed but the control winding is prone to saturation at sub synchronous speed.

Saturation is not a problem at super synchronous speed but the control winding voltage is high as is the voltage rating of the converter.

The best operating characteristics of the BDFTSIM are obtained in the super synchronous speed range, in a narrow band close to the synchronous speed.

#### References

[1] R. Pena, J.C. Clare, G.M. Asher, "Doubly fed induction generator using back-to-back PWM converters and its application to variable speed wind- energy generation", IEEE Proc.-Electr. Power Appl., Vol.143, No.3, 1996, pp231-241

[2] S. Muller, M. Deicke, R.W. De Doncker, "Adjustable Speed Generators for Wind Turbines based on Doubly-fed Induction Machines and 4-quadrant IGBT Converters Linked to the Rotor", IEEE Industry Applications Conference, Vol.4, 2000, pp.2249-2254

[3] B. Hopfensperger, D.J. Atkinson, R.A. Lakin, "Stator flux oriented control of a cascaded doubly-fed induction machine", IEE Proc.-Electr. Power Appl., Vol.146, No.6, 1999, pp597-605.

[4] B. Hopfensperger, D.J. Atkinson, R.A. Lakin, "Combined magnetising flux oriented control of the cascaded doubly-fed induction machine", IEE Proc-Electr Power Appl, Vol.148, No.4, 2001, pp354-362

[5] D. Zhou, R. Spee, G. C. Alexander, "Experimental Evaluation of a Rotor Flux Oriented Control Algorithm for Brushless Doubly-Fed Machines", IEEE Trans. on Power Electronics, Vol.12, No.1, 1997, pp.72-78

[6] G. Boardman, J. G. Zhu, and Q. P. Ha, "General reference frame modelling of the doubly fed induction machine using space vectors", Proc of the Australasian Power Engineering Conference (AUPEC'2002), Melbourne Australia, September 2002

[7] J. G. Zhu, V. S. Ramsden, "Improved formulations for rotational core losses in rotating electrical machines", IEEE Trans. on Magnetics, Vol. 34, No. 4, July 1998, pp. 2234-2242.

[8] D. Basic, J. G. Zhu, G. Boardman, "Modeling and steady state performance analysis of a brushless doubly fed twin stator induction generator", Proc of the Australasian Power Engineering Conference (AUPEC'2002), Melbourne Australia, September 2002

#### Appendix Nomenclature

<i>A</i>	<i>Main Variables</i>
<b>a</b>	Spatial operator $e^{j2\pi/3}$
<i>f</i>	Frequency (Hz)
$\Im$	Imaginary part of complex quantity
<i>j</i>	Imaginary operator
<i>k</i>	Core loss coefficient
<i>L</i>	Inductance (H)
<i>N</i>	Mechanical speed (rpm)
<i>p</i>	Differentiation with respect to time
<i>P</i>	Number of pole pairs
$\wp$	Power (W)
<i>R</i>	Resistance ( $\Omega$ )
$\tau$	Instantaneous torque (Nm)
<i>T</i>	Steady state torque (Nm)
<i>v</i>	Instantaneous voltage (V)
$\theta$	Angular position (rad)
$\omega$	Angular velocity (rad/s)
<i>Z</i>	Impedance ( $\Omega$ )
$\Psi$	Flux linkage (Wb)
<i>B</i>	<i>Subscript and Superscript Variables</i>
<i>a</i>	Anomalous
<i>c</i>	Control machine
<i>e</i>	Eddy current
<i>fe</i>	Iron
<i>g</i>	General
<i>h</i>	Hysteresis
<i>l</i>	Leakage
<i>m</i>	Mechanical
<i>p</i>	Power machine
<i>r</i>	Rotor
<i>s</i>	Stator
*	Complex conjugate

Subscript *m* relating to a magnetic quantity means mutual or magnetizing.

Bold lower case variable denotes instantaneous space phasor. Power winding refers to the stator winding of the power machine and control winding refers to the stator winding of the control machine.